

PAPER • OPEN ACCESS

Assessing the distribution and variation characteristics of marine primary productivity in the coastal marine area of Vietnam South Centre

To cite this article: Nguyen Trinh Duc Hieu *et al* 2022 *IOP Conf. Ser.: Earth Environ. Sci.* **964** 012011

View the [article online](#) for updates and enhancements.

You may also like

- [Nitrogen and carbon limitation of planktonic primary production and phytoplankton–bacterioplankton coupling in ponds on the McMurdo Ice Shelf, Antarctica](#)
Brian K Sorrell, Ian Hawes and Karl Safi
- [The Stripe 82 Massive Galaxy Project. III. A Lack of Growth among Massive Galaxies](#)
Kevin Bundy, Alexie Leauthaud, Shun Saito *et al.*
- [THE STRIPE 82 MASSIVE GALAXY PROJECT. I. CATALOG CONSTRUCTION](#)
Kevin Bundy, Alexie Leauthaud, Shun Saito *et al.*



The Electrochemical Society
Advancing solid state & electrochemical science & technology

243rd ECS Meeting with SOFC-XVIII

More than 50 symposia are available!

Present your research and accelerate science

Boston, MA • May 28 – June 2, 2023

[Learn more and submit!](#)

Assessing the distribution and variation characteristics of marine primary productivity in the coastal marine area of Vietnam South Centre

Nguyen Trinh Duc Hieu^{1,2,3}, Nguyen Huu Huan^{1,4}, Tran Thi Van^{2,3*},
Nguyen Phuong Lien⁵

¹ Institute of Oceanography, Vietnam Academy of Science and Technology (VAST)

² Faculty of Environment and Natural Resources, Ho Chi Minh City University of Technology, (HCMUT), 268 Ly Thuong Kiet Street, District 10, Ho Chi Minh City, Vietnam

³ Vietnam National University Ho Chi Minh City, Linh Trung Ward, Thu Duc District, Ho Chi Minh City, Vietnam

⁴ Graduate University of Science and Technology, Vietnam Academy of Science and Technology (VAST)

⁵ Coastal Branch, Vietnam – Russia Tropical Centre

*tranthivankt@hcmut.edu.vn

Abstract. Primary production (PP) of phytoplankton plays an essential role in food web dynamics, biogeochemical cycles and marine fisheries. It is used as one of the basic information for evaluating marine ecosystems. In this paper, monthly composite PP data on a 4 km x 4 km grid for the period 2003-2020 was used to evaluate the distributional characteristics of PP in the coastal marine area of Vietnam South Centre. The statistical results show that the climatological average of PP in 18 years reached 449.2 mgC/m²/day, ranged from 272.1 to 14,205.4 mgC/m²/day. The PP has seasonal and spatial variations. In time, the lowest value of PP was in spring, and the highest was in winter; in space, PP tended to decrease from shore to offshore, PP was higher in coastal areas than in the open sea areas. During the northeast monsoon season, PP increased by more than 1000 mgC/m²/day in the coastal area. Meanwhile, in the southwest monsoon season, due to the ecological influence of the upwelling phenomenon, PP increased with a value greater than 1500 mgC/m²/day, distributed along the coastline of Ninh Thuan - Binh Thuan. Primary productivity positively correlated with chlorophyll content but negatively correlated with sea surface temperature with correlation coefficients of 0.9 and -0.6, respectively. There was a weak correlation between PP and ONI with correlation coefficients of -0.23. The temporal-spatial variation of PP was affected by the ENSO (El Niño-Southern Oscillation) phenomenon, the positive phase of ENSO (El Niño conditions) corresponded to lower PP, and the negative phase of ENSO (La Niña conditions) corresponded to higher PP. The research results from this paper can be used as a reference in marine ecosystem management.

1. Introduction

Ocean primary production (PP) plays an essential role in the global carbon cycle, and the earth environmental system constitutes roughly half of the biosphere net PP [1]. The value of PP is used as an



Content from this work may be used under the terms of the [Creative Commons Attribution 3.0 licence](https://creativecommons.org/licenses/by/3.0/). Any further distribution of this work must maintain attribution to the author(s) and the title of the work, journal citation and DOI.

indicator of environmental quality and ecological conditions in seawater [2, 3]. Besides that, primary productivity is the base of the food web in marine ecosystems, and it influences the nature of marine food webs and the abundance of marine organisms. It is the ultimate source of energy for all organisms in an ecosystem [4, 5]. However, long-term variability in PP has not been explored [6]. Traditional ship-based in situ measurements are limited in their ability to capture PP large scale spatial and temporal dynamics and are time-consuming and expensive [7, 8]. While remote sensing data can be used to observe the dynamics of the ocean surface, providing fundamental means for estimating oceanic PP on large spatiotemporal scales [9]. One of the essential applications of ocean colour data has been in the PP computation at large scales, using remotely sensed fields of phytoplankton biomass [4]. Today, PP in global and regional scales can be estimated by combine remote sensing techniques and mathematic modelling. Many satellite-based PP models have been used to calculate PP in the ocean in recent years, and they are classified into 3 categories: chlorophyll-based, carbon-based and phytoplankton absorption-based models. The Vertically Generalized Production Model (VGPM) is a chlorophyll-based model whose photosynthesis rate is expressed as a function of water depth and photosynthetically active radiation, and it is used to estimate regional and global ocean PP [10].

Several studies have used remote sensing data to assess the distribution and variation of primary productivity in the East Sea (ES). Tan and Shi, 2009 [11] examined the spatio-temporal variability of ocean PP in the ES for 1998-2006 using the VGPM model. Liao et al., 2012 [12] investigated the interannual variations of PP associated with two different types of Niño in the ES using more than ten years of satellite-derived PP data. Zhou et al., 2017 [13] estimated the primary and the average monthly data of marine primary productivity in 8 days, a detailed analysis of the differences in the 2006-2015 PP in the traditional fishing areas in the ES on the interannual and seasonal variation and spatial distribution. Xu et al., 2017 [14] used Moderate Resolution Imaging Spectroradiometer (MODIS) data to evaluate spatio-temporal variation of PP for the open ES. These studies have shown that peaks in average PP in the ES appeared in winter and summer, with the winter peak more significant than the summer peak [11]. ENSO and physicochemical environmental conditions influence PP spatial and temporal variability in the ES [11, 12]. The spatial distribution of PP in ES also indicated that the PP values are high in shallow offshore areas and then decreasing with the increasing distance away from the coast [14]. The VGPM model was suitable for PP estimation in the central-western East Sea [13].

Using remote sensing data to calculate the distribution of primary productivity in the coastal marine area of Vietnam South Centre was first published by Nguyen Tac An and Tong Phuoc Hoang Son in 2004 [3]. They used ocean colour images to calculate the distribution of primary productivity in the upwelling region in the Southcentral region of the Vietnam sea. The studied results showed that the distribution trend of primary productivity we have from remote sensing technique is similar to other study results and direct measurements in this sea region. In 2012 and 2014, Phan Minh Thu et al. used MODIS Aqua data to evaluate marine primary productivity in the Vietnam sea. The result showed that the upwelling phenomenon impacted PP distribution suspended sediment from Mekong River nutrients supporting human activities [15, 16]. These studies also indicated that remote sensing data could potentially estimate primary productivity in Vietnamese marine regions.

The coastal marine area of Vietnam South Centre is an area of particular importance to Vietnam marine economy. In addition, this area is affected by upwelling during the southwest monsoon season [17]. During upwelling occur, water that rises to the surface is typically colder and rich in nutrients. These nutrients are used by phytoplankton to increase the primary productivity of the oceanic region. So reasonable fishing grounds typically are found where upwelling is common. Therefore, using remote sensing data sources to monitor the distribution and PP fluctuations in this area is a practical matter to be implemented.

In this paper, empirical spatio-temporal mean and cross-correlation function analysis was conducted to accomplish the purposes: (1) Identifying the distribution and variation characteristics of PP; (2) Determining the correlation between PP and chlorophyll-a (chl-a), sea surface temperature (SST),

ENSO phenomenon in the coastal marine area of Vietnam South Centre for a period of 18 years (2003-2020). The results of this article can be used to provide a scientific basis for socio-economic development planning and propose solutions to protect and develop the marine ecosystem sustainably

2. Study area

The study area is the coastal marine zone of Vietnam South Centre, between latitude 10.30° to 16.25° N and longitude 107.30° to 112.00° E. The studied area is shown in Figure 1. The study area is influenced by winter monsoon (northeast monsoon) and summer monsoon (southwest). The interaction of the atmospheric-oceanic processes with the bottom topography and the coast has formed a substantial upwelling area from Khanh Hoa to Binh Thuan waters during the southwest monsoon season, forming fishing grounds with high benefits in fish and molluscs [18]. During upwelling-active phases, cold water from deep towards the ocean surface, causing the SST to drop significantly [19].

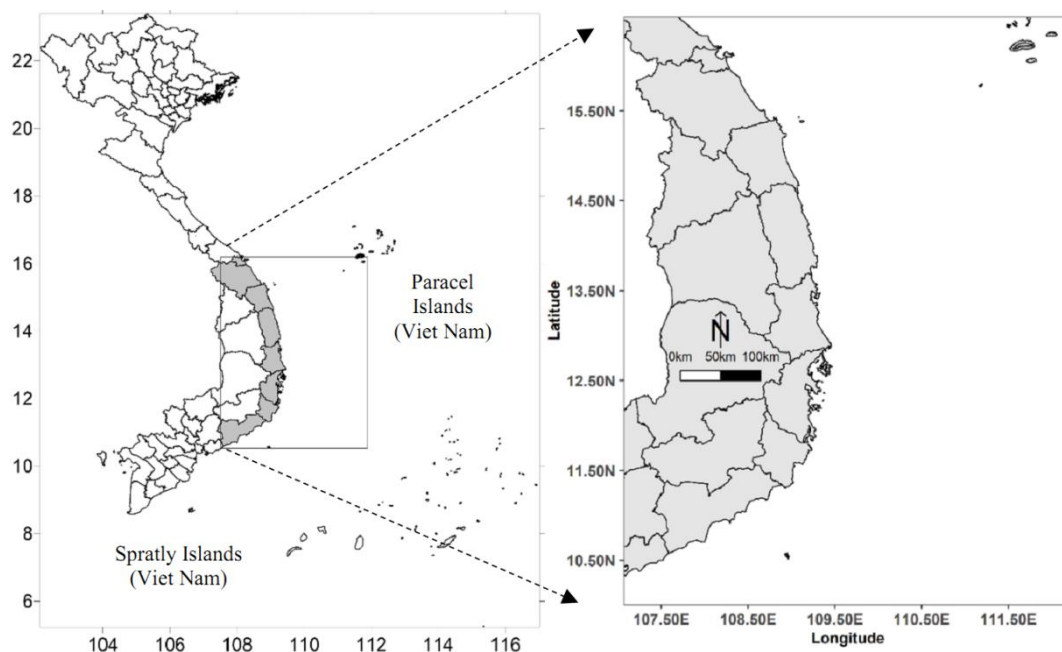


Figure 1. Map showing the study area

3. Data and Methods

The block diagram of the research method in this paper is shown in Figure 2. Accordingly, after determining the research objectives, three types of data are collected as follows: (1) PP data; (2) SST and chl-a data; and (3) Multivariate ENSO Index (MEI) and Oceanic Niño Index (ONI). The collected data source was used to carry out the following two research contents: (1) Analysis of spatial-temporal distribution characteristics; and (2) analyze the possible relationship between PP and chl-a, SST and ENSO phenomenon. To achieve the above two contents, this study uses the following two methods: (1) calculate empirical spatial and temporal mean of PP; and (2) correlation analysis.

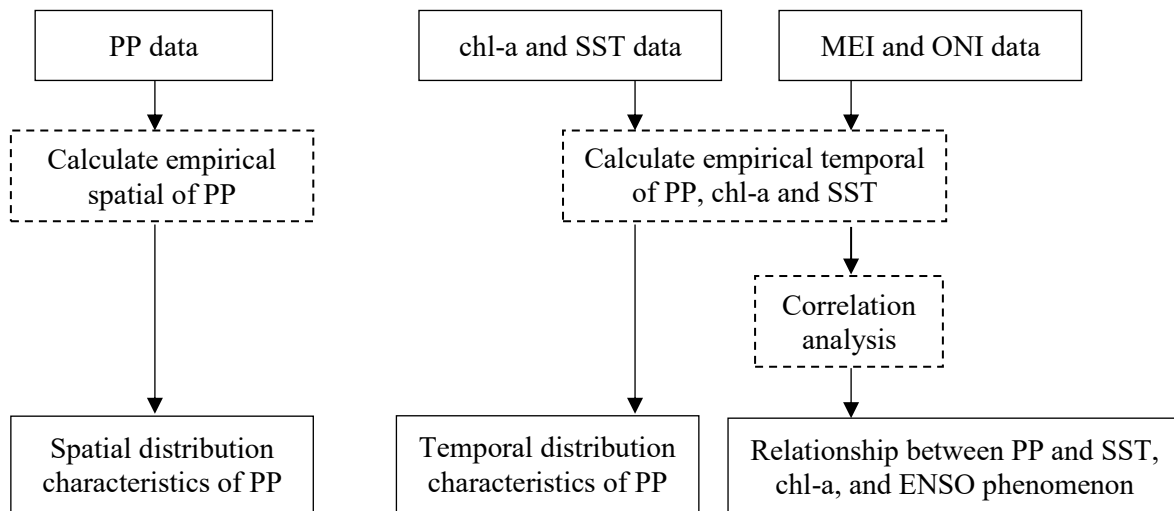


Figure 2. The block diagram of the research method

3.1. Data

In this study, monthly gridded data during 2003-2020 on PP with a spatial resolution of 4 km were from the standard Vertically Generalized Production Model by Behrenfeld and Falkowski (1997) using MODIS Aqua data, provided by National Oceanic and Atmospheric Administration – NOAA (<https://coastwatch.pfeg.noaa.gov/erddap>).

To discuss the relationship between the oceanographic environment and PP, we used monthly averaged chl-a and SST with 4 km x 4 km spatial resolution from Level-3 Standard Mapped Image products observed by the MODIS Aqua satellite. Chl-a concentration and SST data were provided by the National Aeronautics and Space Administration Ocean Color Web site (<https://oceancolor.gsfc.nasa.gov/>).

To assess the impact of ENSO on the PP over the coastal marine area of Vietnam South Centre, monthly time series of two climate indices ONI (Oceanic Niño Index) and MEI (Multivariate ENSO Index) during 2003-2020, was derived from National Oceanic and Atmospheric Administration (<http://www.esrl.noaa.gov/psd/enso/>). The ONI is NOAA primary indicator for monitoring El Niño and La Niña, which are opposite phases of the climate pattern called the El Niño-Southern Oscillation, or “ENSO” for short. NOAA considers El Niño conditions present when the Oceanic Niño Index is +0.5 or higher, indicating the east-central tropical Pacific is significantly warmer than usual. La Niña conditions exist when the Oceanic Niño Index is -0.5 or lower, indicating the region is cooler than usual. The MEI is the bi-monthly time series of the leading combined empirical orthogonal function of five different variables, namely, sea level pressure, sea surface temperature, the surface wind of combined zonal and meridional components, and outgoing longwave radiation, over the tropical Pacific basin (30°S-30°N and 100°E-70°W). Summary of data in this paper is shown in Table 1.

The global PP, chl-a and SST data with netCDF format were preprocessed, including reading, image cropping, calculating average in R programming language, which were cropped by the scope of the studying area.

Table 1. Summary of data in the study

Name	Product type	Time period of data	Data source
PP	4 km resolution monthly grid data	From 1/2003 to 12/2020	https://coastwatch.pfeg.noaa.gov/erddap
chl-a and SST			https://oceancolor.gsfc.nasa.gov/
MEI and ONI	Monthly time series data		http://www.esrl.noaa.gov/psd/enso/

3.2. Methods

3.2.1. Calculate empirical spatial and temporal mean

Assume for the moment that we have observations $\{PP(s_i; t_j)\}$ for spatial locations $\{s_i; i = 1, 2, \dots, m\}$ and times $\{t_j; j = 1, 2, \dots, T\}$. The empirical spatial mean for location $\mu_{z,s}(s_i)$ is then found by averaging over time by equation 1 [20]:

$$\mu_{z,s}(s_i) = \frac{1}{T} \sum_{j=1}^T PP(s_i; t_j) \quad (1)$$

where T is the time used to calculate the empirical spatial mean.

The empirical temporal mean for time $\mu_{z,s}(t_j)$, is given by equation 2 [20]:

$$\mu_{z,s}(t_j) = \frac{1}{m} \sum_{i=1}^m PP(s_i; t_j) \quad (2)$$

where m is the number of pixels of each scene.

Based on the data results of PP, the spatial monthly mean of PP were exported to raster and then mapping and visualization in R software.

3.2.2. Correlation analysis

Pearson correlation analysis was used to measure the statistical relationship between PP and chl-a, SST, ONI, MEI, and further to evaluate the impact of ENSO on the distribution and variability of PP. Pearson correlation coefficient (r) in the range from -1 (anti-correlation) to $+1$ (perfect correlation), between these two monthly time series x and y , with N elements as equation 3 [9]:

$$r = \frac{\sum_{i=1}^N (x_i - \bar{x})(y_i - \bar{y})}{\sqrt{\sum_{i=1}^N (x_i - \bar{x})^2} \sqrt{\sum_{i=1}^N (y_i - \bar{y})^2}} = \frac{\text{Cov}(x,y)}{\sigma_x \sigma_y} \quad (3)$$

with Cov being the covariance function, \bar{x} and \bar{y} the average and σ_x and σ_y the standard deviations for x and y , respectively.

Besides that, cross-correlation function (CCF) analysis was also used to describe and model the relationship between two time series. In the relationship between two time series (y_t and x_t), the series y_t may be related to past lags of the x -series. The cross-correlation function helps identify lags of the x -variable that might be useful predictors of y_t [21]. The sample cross-correlation function is defined as the set of sample correlations between x_{t+h} and y_t for $h = 0, \pm 1, \pm 2, \pm 3, \dots$. A negative value for h correlates the x -variable before t and the y -variable at time t . For instance, consider $h = -2$. The CCF value would give the correlation between x_{t-2} and y_t . When one or more x_{t+h} , with h negative, are predictors of y_t , x leads y . When one or more x_{t+h} , with h positive, are predictors of y_t , x lags y . In this paper, x represents ONI/MEI, and y represents the PP value. This method used ONI/MEI to forecast fluctuations (increase/decrease) of the PP value.

All the graphs, calculations, and statistical analyses were performed using R software.

4. Result and Discussion

4.1. Spatial-temporal distribution and variation characteristics of PP

The statistical results show that the climatological average of PP in 18 years reached $449.2 \text{ mgC/m}^2/\text{day}$, ranged from 272.1 to $14,205.4 \text{ mgC/m}^2/\text{day}$. The monthly mean PP varied significantly between months in this study area reached the highest value in January with $578.5 \text{ mgC/m}^2/\text{day}$, and the lowest PP in May with the value of $320.3 \text{ mgC/m}^2/\text{day}$ (Figure 3A). This result is similar to the monthly variation of multiyear averaged PP in the ES reported by Tan and Shi, 2009 [11].

In Figure 3A the PP reached 2 maximum peaks: one strong peak in winter (January) and one weak in summer (August). The winter peak was more significant than the summer, similar to previous studies in the ES [11, 22]. Previous research also showed that in the coastal marine area of Vietnam South Centre, the primary productivity in summer and winter is higher due to the eastern shelf and the Mekong River [13]. This paper said that PP seasonal distribution also indicates that PP reached the highest value in winter and lowest in spring, similar to Xu et al., 2017 [14] and Tan and Shi, 2009 [11].

Figure 3B showed the annual mean values of PP in 2003-2020 with the maximum value in 2011 and the minimum value in 2010 with corresponding values of 500 mgC/m²/day and 370.9 mgC/m²/day, respectively. Yearly averaged PP had the lowest values during the summer of 2010. This anomalous event coincided with the 2009-2010 El Niño event. Meanwhile, the maximum PP value in the winter of 2011 coincided with the strong La Niña phenomenon in 2010-2011. Research by Zhou et al., 2017 [13] also showed that in the western part of the ES between 2006 and 2015, PP reached the maximum value in 2011 and the minimum value in 2010.

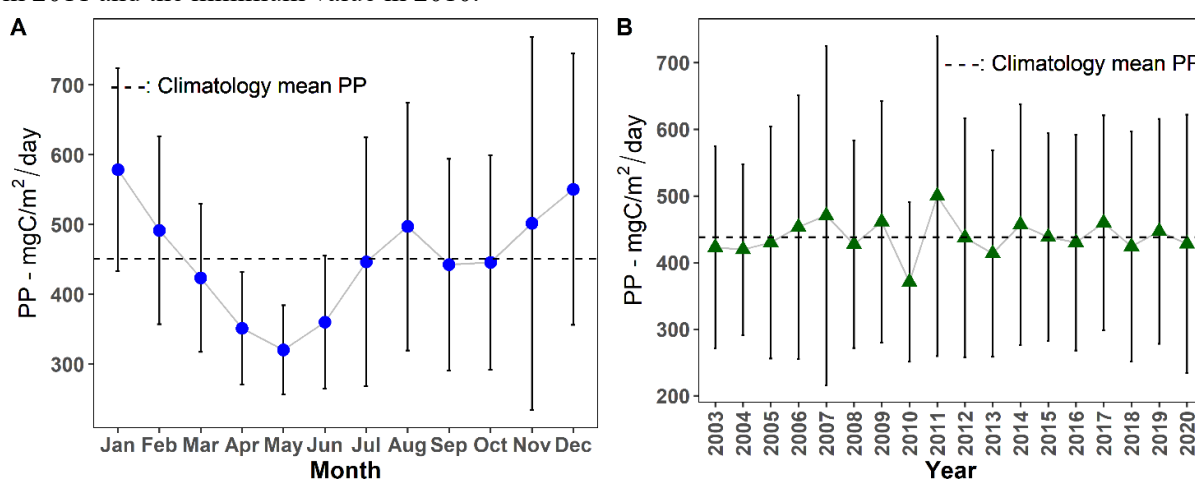


Figure 3. Monthly (A) and yearly (B) average variations of mean PP (mgC/m²/day) from 2003-2020

The spatial distribution results of the monthly mean value of PP over the past 18 years are listed in Figure 4. It tended to decrease from shore to offshore. PP was higher in coastal areas than in the open sea areas. The lowest levels of PP were identified during spring (March to May), and the region with high PP levels was limited to a very narrow band near the coast in the north of the coastal marine area of Vietnam South Centre (15° – 16°N). Spring is the transition period between northeast monsoon to southwest monsoon, low levels of PP may be related to mixed layer depth. According to the discussion of Tan and Shi, 2009 [11] indicated that the mixed layer depth of ES is the shallowest in spring (< 20 m) and deepest in winter (35 - 40 m).

The average PP level in the south of the study area increases significantly in summer, although the average PP level from the coast of Da Nang to the coast of Khanh Hoa was still low. In the southwest monsoon season (June to August), due to the ecological influence of the upwelling phenomenon, PP increased with a value greater than 1,500 mgC/m²/day, distributed along the coastline of Ninh Thuan - Binh Thuan (Figure 4). High PP appears as a large jet, extending from the coastal waters of Ninh Thuan-Binh Thuan northeastward during the annual southwest monsoon. A previous study showed that this jet of high PP in this study area was associated with coastal upwelling driven by the southwest monsoon and discharges from the Mekong River [11]. The phenomenon of coastal upwelling brought nutrients from the subsurface to the surface, and Mekong River discharge delivers a high flux of nutrients from the continent and into the sea. These nutrients are used by phytoplankton to increase the primary productivity of the coastal marine area of Vietnam South Centre.

The PP levels increased in autumn along the coastline in the study area during autumn (September to November). PP values decreased with the increasing distance away from the coast (Figure 4). During the northeast monsoon period (December to February of the following year), PP increased with a concentration larger than 1,000 $\text{mgC}/\text{m}^2/\text{day}$ along a narrow strip of shallow water adjacent to the coastline for the whole study area (109.50°E back to shore) (Figure 4). During winter, the northeast monsoon reached its strongest level, increasing the mixed layer depth and bringing nutrient-rich water to the surface, allowing PP to rise to highly elevated levels, the highest in winter [11].

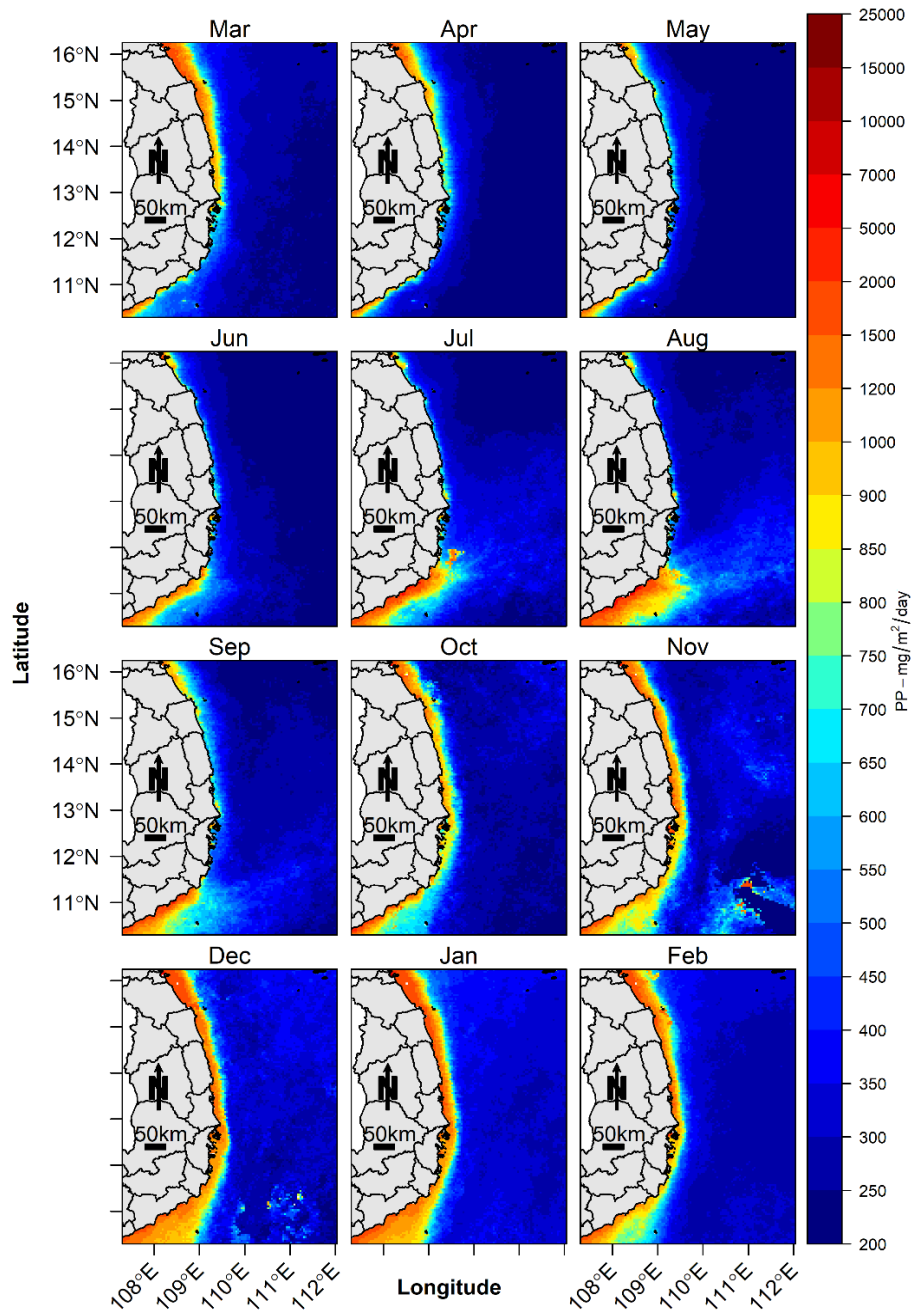


Figure 4. Monthly mean climatology maps of PP ($\text{mgC}/\text{m}^2/\text{day}$) in the period 2003-2020

4.2. Correlation between PP and SST, chl-a, ENSO

The spatial-temporal variation of PP is influenced by environmental conditions such as chl-a and SST. There exists a negative correlation between PP and SST, with the correlation coefficient reached -0.6 (Pearson test, $P < 0.05$), previous research has also shown that PP and SST showed an excellent inverse correlation with a correlation coefficient equal to -0.8 [11]. This correlation revealed that anomaly high/low SST was associated with anomaly low/high PP levels. Availability of SST is a crucial factor limiting the distribution of PP. However, Tan and Shi, 2009 [11] showed that in the ES, the change of SST is not the cause that directly affects the change of PP. It has shown that, although there exists an inverse relationship between SST and PP, low SST is not the limiting cause of PP. As analyzed above, the southwest and northeast monsoon winds influence a change of SST and PP concentration. The strong monsoon winds affect the movement changes the value of the SST, and affect the mixing of water masses vertically related to the concentration of PP. Some factors such as monsoon winds, upwellings, and river discharges must significantly control phytoplankton biomass and primary productivity by changing the transport and distribution of nutrient-rich water. The above analysis shows that the availability of nutrients can be one of the reasons for limiting PP value in the coastal marine area of Vietnam South Centre.

Meanwhile, PP and chl-a have a significant positive correlation with a correlation coefficient equal to 0.9 (Pearson test, $P < 0.05$). Chlorophyll-a concentration has been invoked to indicate both PP (a flux) and phytoplankton biomass (a scalar). Besides, the VGPM is a “chlorophyll-based” model that estimates net PP from chlorophyll-a content. Thus, an increase/decrease in chl-a level leads to an increase/decrease in PP value. The results of this correlation analysis have shown that in the period from 2003 to 2020, low PP appeared with low chl-a, and high PP appeared with high chl-a.

The results of the correlation analysis also showed that there was no linear correlation between PP and MEI (Pearson test, $r = -0.13$, $P > 0.05$). However, there was a weak correlation between PP and ONI (Pearson test, $P < 0.05$). The correlation of PP and ONI showed a significant negative correlation ($r = -0.23$, $P < 0.05$), which suggested that ENSO was probably the dominant factor that drove PP variation in this study area. The correlation coefficient between ONI and PP is low, indicating that ENSO influence against the PP which seen from the correlation value is not too large. Based on the relationship between ONI and PP, the ONI was used to forecast the fluctuation of the PP value. Cross-correlation function analysis showed that the most dominant cross-correlations occur between $h = -6$ and about $h = 3$ (Figure 5). There are nearly equal maximum values at $h = 0$, -1, and -2, with tapering occurring in both directions from that peak. The correlations in this region ($h = 0$, -1, -2) are negative, indicating that an increase (decrease) in the ONI value leads to a decline (increase) in the PP value with a phase difference of about 0 to 2 months (ONI ahead) (Figure 5). This result indicated that PP values fluctuate (increase or decrease) after the occurrence of the ENSO phenomenon about 0 to 2 months.

The monthly time series of the PP and ONI were displayed in Figure 6. The correlation coefficient between PP and ONI has shown that PP is negatively correlated with ONI. That is, the positive phase of ENSO (El Niño conditions) corresponded to lower PP, and the negative phase of ENSO (La Niña conditions) corresponded to higher PP, the correlation between PP and ENSO in this study is consistent with previous studies in East Sea [23]. This result can be explained because the ENSO phenomenon influences the summer and winter monsoon. The intensity of the East Sea summer monsoon tends to be weaker (stronger) in years associated with a warm (cold) ENSO event [24]. Besides that a weak East Asian winter monsoon also generally links to an El Niño event. At the same time, a strong one corresponds to a La Niña event in the tropical eastern Pacific [25]. The weakened winter monsoon leads to a decrease in the depth of the mixed layer and decreases upward nutrient flux, and the weakened summer monsoon leads to weak upwelling and reduced upward nutrient flux.

The time-series graph of the ONI in Figure 6 indicated that in the period from 2003 to 2020, the ONI value reached 2 minimum peaks corresponding to 2 La Niña times in 2007-2008 and 2010-2011. Observing time series data of PP in Figure 6 showed that PP reached its highest value in November 2007 with a value of about 1,409 mgC/m²/day due to the influence of strong La Niña in 2007. Besides, the La

Niña event of 2007-2008 also affected the abnormal increase in PP during the period from October 2007 to February 2008. Meanwhile, the La Niña phenomenon in 2010-2011 caused an increase in PP value from October 2010 to March 2011 with a maximum peak of 669 mgC/m²/day in January 2011.

Besides the 2 minimum peaks, Figure 6 also showed that ONI reached 2 maximum peaks during El Niño in 2009-2010 and 2015-2016. The 2009-2010 El Niño event caused not only a decrease in PP value in the winter of 2009 but also a decrease in PP in the summer of 2010 with minimum values of 417 mgC/m²/day in February 2010 and 295 mgC/m²/day in June 2010, respectively. El Niño phenomenon in 2015-2016 also caused an abnormal decrease in PP value from October 2015 to January 2016, with the minimum PP value reaching 333 mgC/m²/day in November 2015.

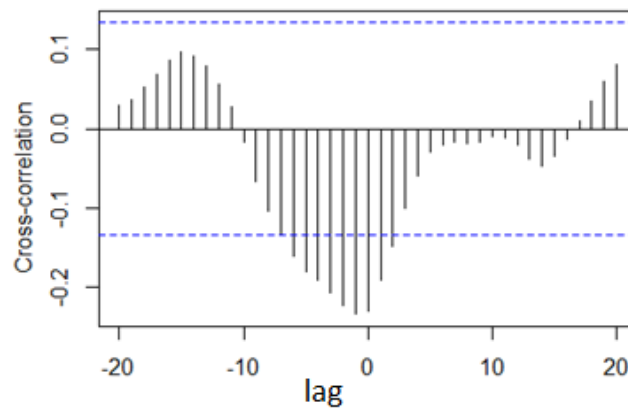


Figure 5. Cross-correlation function of ONI and PP (dotted lines are 95% confidence intervals)

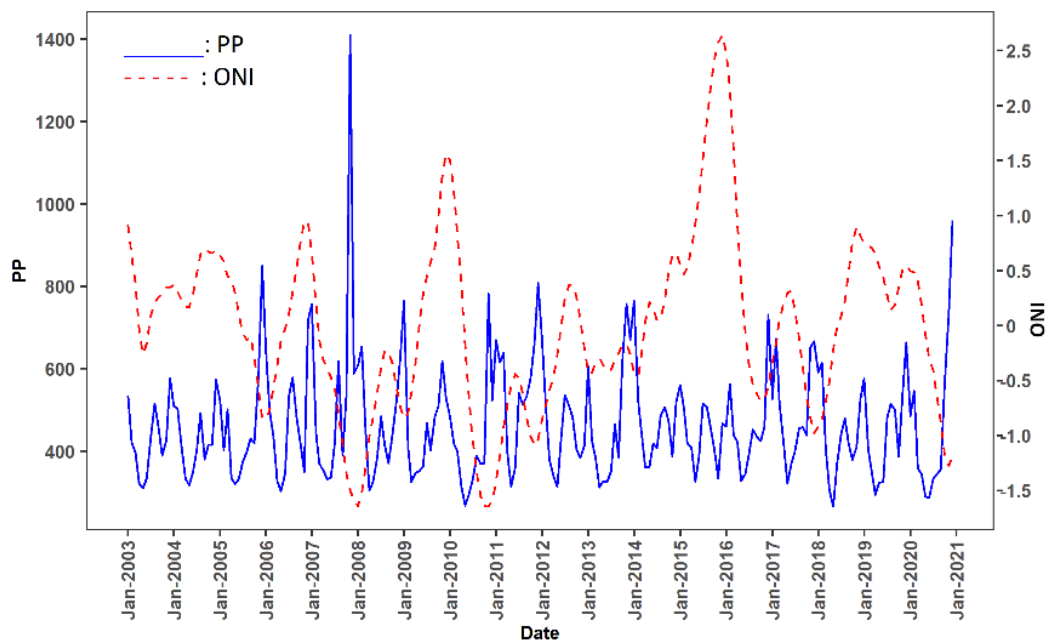


Figure 6. Time series of mean PP (mgC/m²/day) (blue line) and ONI (red line) in the period of 2003-2020

5. Conclusion

The monthly mean PP varied significantly between months (highest in January, lowest in May), seasons (maximum peak in winter and minimum peak in spring) and years (highest in 2011 and lowest in 2010) in the coastal marine area of Vietnam South Centre during the period of 2003-2020. The spatial distribution of PP tended to decrease from shore to offshore, and PP was higher in coastal areas than in the open sea areas. The increase in PP value in winter and summer is due to the influence of northeast monsoon and southwest monsoon, respectively.

PP was positively correlated with chl-a and negatively correlated with SST with Pearson correlation coefficients of 0.9 and -0.6, respectively. PP also had a weak statistically significant correlation with ONI with a correlation coefficient of -0.23, so that ENSO influence against the PP which seen from the correlation value is not too large. The ENSO phenomenon affected the spatio-temporal variation of PP, the positive phase of ENSO corresponded to lower PP, and the negative phase of ENSO corresponded to higher PP, with a phase difference of about 0 to 2 months (ONI ahead).

Acknowledgements

The authors thank project 01/ĐTT-STB-2021 for the support of facilities for this study. We would like to thank Ho Chi Minh City University of Technology (HCMUT), VNU-HCM for the support of time and facilities for this study.

This paper is a contribution to celebrate the 100 years Anniversary of the Institute of Oceanography, Vietnam Academy of Science and Technology

References

- [1] Field, C.B., M.J. Behrenfeld, J.T. Randerson, and P. Falkowski, 1998 Primary production of the biosphere: integrating terrestrial and oceanic components. *Science*, 281(5374), 237-240.
- [2] Li, H., H. Peng, M. Sun, J. Liang, and H. Yao, 2009 The study on dynamic changes of NPP in coastal ocean of China. *Remote Sensing of the Ocean, Sea Ice, and Large Water Regions 2009*. International Society for Optics and Photonics.
- [3] Nguyen Tac An and Tong Phuoc Hoang Son, 2004 Application of Remote Sensing for Interpretation of Primary Productivity in Bien Dong (Eastern Sea). *Proceedings of the Geoinformatics for Spatial-Infrastructure Development in Earth and Applied Sciences (GIS-IDEAS 2004)*.
- [4] Lakshmi, E., D. Pratap, P. Nagamani, K. Rao, T.P. Latha, and S. Choudhury, 2014 Time Series Analysis Of Primary Productivity Along The East Coast Of India Using Oceansat-2 Ocean Colour Monitor (OCM). *The International Archives of Photogrammetry, Remote Sensing and Spatial Information Sciences*, 40(8): p. 1049.
- [5] Son, S., M. Wang, and L.W. Harding Jr, 2014 Satellite-measured net primary production in the Chesapeake Bay. *Remote sensing of environment*, 144: p. 109-119.
- [6] Liu, G. and F. Chai, 2009 Seasonal and interannual variability of primary and export production in the South China Sea: a three-dimensional physical–biogeochemical model study. *ICES Journal of Marine Science*, 66(2): p. 420-431.
- [7] Tin, H.C., M.W. Lomas, and J. Ishizaka, 2016 Satellite-derived estimates of primary production during the Sargasso Sea winter/spring bloom: Integration of in-situ time-series data and ocean color remote sensing observations. *Regional Studies in Marine Science*, 3: p. 131-143.
- [8] Carr, M.-E., M.A. Friedrichs, M. Schmeltz, M.N. Aita, D. Antoine, K.R. Arrigo, I. Asanuma, O. Aumont, R. Barber, and M. Behrenfeld, 2006 A comparison of global estimates of marine primary production from ocean color. *Deep-Sea Research Part II: Topical Studies in Oceanography*, 53(5-7): p. 741-770.
- [9] Li, W., S.P. Tiwari, H.M. El-Askary, M.A. Qurban, V. Amiridis, K. ManiKandan, M.J. Garay, O.V. Kalashnikova, T.C. Piechota, and D.C. Struppa, 2020 Synergistic Use of Remote Sensing and Modeling for Estimating Net Primary Productivity in the Red Sea With VGPM, Eppley-

- VGPM, and CbPM Models Intercomparison. *IEEE Transactions on Geoscience and Remote Sensing*.
- [10] Behrenfeld, M.J. and P.G. Falkowski, 1997 Photosynthetic rates are derived from satellite-based chlorophyll concentration. *Limnology and Oceanography*, 42(1): p. 1-20.
- [11] Tan, S.C. and G.Y. Shi, 2009 Spatiotemporal variability of satellite-derived primary production in the South China Sea, 1998–2006. *Journal of Geophysical Research: Biogeosciences*, 114(G3).
- [12] Liao, X., J. Ma, and H. Zhan, 2012 Effect of different types of El Niño on primary productivity in the South China Sea. *Aquatic Ecosystem Health & Management*, 15(2): p. 135-143.
- [13] Zhou, W., H. Xu, A. Li, and S. Ji, 2017 Zone statistics of the oceanic primary productivity for the traditional fishing areas of the open South China sea based on MODIS products. *Applied Ecology And Environmental Research*, 15(3): p. 1013-1024.
- [14] Xu, H., W. Zhou, A. Li, and S. Ji, 2016 Similarities and differences of oceanic primary productivity product estimated by three models based on MODIS for the open South China Sea. *International Conference on Geo-Informatics in Resource Management and Sustainable Ecosystem*. Springer.
- [15] Thu, P.M., N.H. Huan, L.T. Dung, L.T. Dung, V.H. Thi, T.T.M. Hue, and H.T. Du, 2014 Primary productivity of phytoplankton in Van Phong Bay, Khanh Hoa province, Vietnam. *Collection of Marine Research Works*, 20.
- [16] Minh Thu, P., N. Manh Tien, N.H. Thai Khang, and L. Va Khin, 2012 Photosynthesis of phytoplankton in the southern marine regions of Vietnam from MODIS data. *International Symposium on Geoinformatics for Spatial Infrastructure Development in Earth and Allied Sciences 2012*.
- [17] Bui Hong Long, 2009 The phenomenon of water upwelling in the sea of Vietnam. *Natural Science and Technology Publishing House*.
- [18] Trinh Thi Minh Trang, Nguyen Thi Nguyet Ha, Tran Duc Thanh, 2015 The positional resources of Khanh Hoa coast: Potentials and Prospects. *Journal of Marine Science and Technology*, 15(1): p. 13-24.
- [19] Bui Hong Long, 2011 Handbook of search on natural conditions, ecological environment, economy, society and integrated management of the South Central Coastal zone. *Natural Science and Technology Publishing House*.
- [20] Cressie, N. and C.K. Wikle, 2015 Statistics for spatio-temporal data. *John Wiley & Sons*.
- [21] Shumway, R.H. and D.S. Stoffer, 2017 Time series analysis and its applications: with R examples. *Springer*.
- [22] Liu, K.-K., S.-Y. Chao, P.-T. Shaw, G.-C. Gong, C.-C. Chen, and T. Tang, 2002 Monsoon-forced chlorophyll distribution and primary production in the South China Sea: observations and a numerical study. *Deep-Sea Research Part I: Oceanographic Research Papers*, 49(8): p. 1387-1412.
- [23] Ma, W., F. Chai, P. Xiu, H. Xue, and J. Tian, 2013 Modelling the long-term variability of phytoplankton functional groups and primary productivity in the South China Sea. *Journal of oceanography*, 69(5): p. 527-544.
- [24] Zhou, W. and J.C. Chan, 2007 ENSO and the South China Sea summer monsoon onset. *International Journal of Climatology: A Journal of the Royal Meteorological Society*, 27(2): p. 157-167.
- [25] Zhou, W., W. Chen, and D.X. Wang, 2012 The implications of El Nino-southern oscillation signal for south China monsoon climate. *Aquatic Ecosystem Health & Management*, 15(1): p. 14-19.